J. Physiol. (1977), **269**, *pp.* 155–176
With 2 plates and 7 text-figures
Printed in Great Britain

ACETYLCHOLINE RECEPTOR DISTRIBUTION ON MYOTUBES IN CULTURE CORRELATED TO ACETYLCHOLINE SENSITIVITY

BY B. R. LAND, T. R. PODLESKI, E. E. SALPETER AND M. M. SALPETER

From the Section of Neurobiology and Behavior, Department of Physics, and School of Applied and Engineering Physics, Cornell University, Ithaca, New York 14853, U.S.A.

(*Received 21 December 1976*)

SUMMARY

1. A linear relation, with a slope of $0{\cdot}9 \pm 0{\cdot}2$ on a log–log plot, was obtained between acetylcholine (ACh) sensitivity and α-bungarotoxin (α-BTX) binding site density in developing L6 and rat primary myotubes. ACh sensitivity was defined as g/Q^n where g is conductance, Q is ACh charge and n is the Hill coefficient. Experimentally we found $n \sim 1{\cdot}7$ for our myotubes, which is similar in value to that reported for adult systems.

2. The linear relationship is compatible with an organization whereby each ion channel is always complexed with a fixed number of ACh receptors such that the dose–response characteristics of each such complex are independent of average ACh receptor density.

3. Light microscope autoradiography showed that the α-bungarotoxin binding sites on L6 myotubes are uniformly distributed over the surface, while primary rat myotubes exhibit gradients and hot spots. Electron microscope autoradiography indicated that about 70% of the [^{125}I]α-bungarotoxin label was on the surface of the myotubes.

The α-bungarotoxin site density, after subtracting myoblast background, varied from 5 to 400 sites/μm^2 on different L6 myotubes, and from 54 to 900 sites/μm^2 on primary rat myotubes, with occasional hot spots of 3000–4000 sites/μm^2. The conductance sensitivities varied from 10^{-4} to 2×10^{-2} MΩ^{-1}/nC$^{1{\cdot}7}$.

INTRODUCTION

The distribution of acetylcholine (ACh) sensitivity on skeletal muscle is altered during development. Early in development the ACh response is more or less uniformly distributed on the surface of myotubes with an

overall low sensitivity (Diamond & Miledi, 1962). Subsequently, the ACh response is restricted to the end-plate with considerably higher sensitivity (Axelsson & Thesleff, 1959; Barnard, Dolly, Porter & Albuquerque, 1975; Kuffler & Yoshikami, 1975). The adult end-plate has a high surface site density of acetylcholine receptor (AChR) (Fertuck & Salpeter, 1976; Barnard, Wieckowski & Chiu, 1971) and has a sigmoid ACh dose–response curve (Changeux & Podleski, 1968; Hartzell, Kuffler & Yoshikami, 1975; Rang, 1971). It has been suggested that this sigmoid dose–response curve is a result of AChR interactions (Karlin, 1967; Changeux, Thiery, Tung & Kittel, 1967).

Muscle cells in culture form multinucleated myotubes that resemble embryonic muscle fibres (see reviews by Konigsberg, 1963; Yaffe, 1971). Such myotubes have a low ACh sensitivity along their full length similar to that in embryonic muscle (Steinbach, Harris, Patrick, Schubert & Heinemann, 1973; Fischbach & Cohen, 1973) and are a favoured system for the study of the differentiation of excitable tissue.

The term AChR has been used in different studies to refer both to a single ACh binding site and to a larger unit containing multiple ACh binding sites. We will use the term AChR to refer to a single ACh binding site, measured operationally by α-bungarotoxin binding, and use the term AChR complex to refer to the structure associated with a single ion channel. Such a complex may contain a single or more than one AChR. If more than one AChR subunit is involved in one complex, they must, by this definition, be linked to each other in a fixed structural relation, independent of the over-all average AChR site density.

Three questions we have asked are: (1) how is the development of AChR binding sites related to the appearance of functional AChR sensitivity? (2) is increased ACh sensitivity during development due simply to a greater density of receptors, or is it due to a changed response of individual receptors to ACh? (3) is the sigmoid shape of the ACh dose–response curve due to interaction between adjacent receptor complexes or does it reflect the response characteristics of individual receptor complexes? To answer these questions we measured ACh (α-BTX) binding site density, ACh sensitivity and the shape of the ACh dose–response curve as reflected in the Hill coefficient (see review by Rang, 1971) using myotubes in culture.

Katz & Miledi (1972) and Anderson & Stevens (1973) have shown that each activated ion channel contributes a fixed conductance change and therefore more current flows in direct proportion to the number of ion channels activated. If no interaction exists between adjacent AChR complexes, then ACh sensitivity should be proportional to AChR density, as long as an equal area is intersected by the delivered ACh pulse. Any deviation from proportionality caused by an interaction between nearby

AChR complexes would be expected to be more pronounced at higher ACh site densities.

In the present study, we obtained a range of sensitivities by using both L6 myotubes and primary cultured rat myotubes which generally have higher sensitivities than L6. ACh sensitivity was measured by iontophoretic application of ACh and intracellular recording. The surface density of AChR was measured using quantitative light autoradiography after AChR blockade by ^{125}I-labelled α-BTX. We found that ACh sensitivity was proportional to average AChR density and that the Hill coefficient, and thus the shape of the dose–response curve, was independent of the AChR site density. We conclude that the increase in ACh sensitivity during development of myotubes in culture is due simply to an increased (linearly additive) number of AChR complexes and that the shape of the ACh dose–response curve is not dependent on interaction between adjacent receptor complexes. Any AChR coupling which exists must reside within the individual AChR complexes.

METHODS

Culture procedure

L6 cells (Yaffe, 1968) were raised as previously described (Land, Sastre & Podleski, 1973). Primary rat myoblasts were obtained by mincing the leg muscles of 18-day *in utero* foetal rats after removing paws and bones. The minced muscle was digested for about 1 hr using 0·025 % viokase in Eagle's, dissociated further by pipetting, then filtered through lens paper (Kodak no. 154-6027) into tissue culture dishes containing the normal culture medium, Eagle's plus 10 % foetal calf serum. Loose cells were removed after 4 hr and the medium replaced with fresh medium. Fusion of myoblasts was visible within 3 days.

ACh sensitivity

Electrophysiological measurements were made at room temperature, 19–21° C, in HEPES (*N*-2-hydroxyethyl piperazine-*N*-2-ethane sulphonic acid) buffered Tyrode saline of the following composition (mM): NaCl 138, KCl 2·7, $MgCl_2$ 1·8, $CaCl_2$ 1·8, NaH_4PO_4, 0·42, glucose 5·5, HEPES 18. The pH was adjusted to 7·4 using 1 M-NaOH. Intracellular voltage measurements were made on myotubes using 30–50 MΩ, 3 M-KCl-filled, glass micro-electrodes. Myotube input resistances were determined by the chopped current technique of Brennecke & Lindemann (1971). This technique allows current injection and voltage reading through the same electrode while minimizing the effects of spreading potential and electrode non-linearities. A single electrode was used so as to minimize damage to myotubes.

ACh was applied by iontophoresis from electrodes measuring 90–150 MΩ when filled with 2 M-ACh. A holding current of 2–7 nA was used to stop ACh diffusion from the electrode between release pulses. The level of holding current was adjusted for each myotube. To adjust the holding current, small test doses of ACh were ejected while the holding current was slowly reduced. The resulting peak depolarization per unit of iontophoretic charge passed became progressively larger and the time-to-peak stayed constant until a holding current level was reached at which the time-to-peak and width of the ACh response became larger. This presumably

reflects the point at which the constant ACh leak desensitizes the nearer AChR (Dreyer & Peper, 1974). The holding current was then increased by one nA and this was the level used.

To measure the ACh sensitivity, one ACh electrode was placed 1–4 μm above the myotube and varying amounts of ACh released by ACh current pulses of 10 msec duration. The intracellular peak depolarization (ΔV) was then recorded as a function of the ACh charge (Q) released at the electrode. The released ACh charge (Q) was obtained from the total current pulse (minus the 1 nA adjusted holding current) times the 10 msec pulse duration.

Sensitivity is often expressed as $\Delta V/Q$. There are several difficulties with such a definition. First, depolarization (ΔV) depends on various membrane parameters such as input resistance, inversion potential and resting potential. The parallel channel conductance model (reviewed by Ginsborg, 1973; Fatt & Katz, 1951) for a cell undergoing a slow ACh induced depolarization allows us to express ΔV in terms of conductance change (g), a measure independent of the myotube resting potential and input resistance. This model gives

$$\Delta V = \frac{R_{in} g(E_m - E_a)}{R_{in} g + 1}, \tag{1}$$

where E_m is the resting potential, E_a the inversion potential of ACh induced current, R_{in} the input resistance and g the peak ACh induced conductance change. When rewritten it gives

$$g = \frac{\Delta V}{R_{in}(E_m - E_a - \Delta V_n)}. \tag{2}$$

We and others (Ritchie & Fambrough, 1975; Steinbach, 1975) have found E_a to be approximately zero for L6 and primary rat myotubes, so E_a can be omitted from the equation in the present study.

A difficulty with expressing sensitivity either as $\Delta V/Q$ or as g/Q stems from the commonly obtained S-shaped ACh dose–response curve. Such a dose–response curve means that neither ΔV nor g are linear with Q but, as will be discussed later, $g \propto Q^n$ where n is the Hill constant for non-saturating ACh conditions. Therefore any definition of sensitivity based on a first order function of Q (such as $\Delta V/Q$, g/Q or the function dg/dQ) will give non-constant sensitivity values which vary with Q even for the same membrane.

We will therefore use a definition of sensitivity which gives a value unchanged by varying Q. We call this the conductance sensitivity,

$$S_g = g/Q^n. \tag{3}$$

To get S_g for each myotube we measured the resting potential E_m and the input resistance R_{in}. (The input resistance was measured as the slope of the linear relationship between current injected and change in membrane voltage.) We then measured the peak depolarization ΔV and time-to-peak (t_p) for several values of Q, and obtained the corresponding values of g from eqn. (2). Finally, the response to ACh or conductance sensitivity (S_g) was determined from a plot of log g *vs.* log Q by fitting a line of constant slope, n, to this plot. For n we used the experimentally derived Hill coefficient for our system (see double electrode procedure described below). For any one myotube this line then gives a single best fit value for g/Q^n derived from the full dose–response curve.

To determine the ACh dose–response Hill coefficient, as well as to determine the linearity of the ACh electrodes, two ACh electrodes were used as described by Katz & Thesleff (1957). A sequence of proportionally related doses were produced using the

cell itself as a monitor of ACh release. Releasing ACh from each electrode separately, the ACh currents were adjusted until myotube responses to each pulse were equal. The electrodes were placed close together (2–4 μm apart) and far from the cell (7–10 μm) so virtually the same set of AChR were hit by the two pulses. Equal responses therefore implied equal AChR occupancy and equal concentration of ACh. The ACh electrode currents were set for each electrode separately so that the same response ΔV_1 was obtained when either electrode was pulsed alone. The response of the myotube was thus used to set the ACh dose, A, to be identical for the two electrodes, even though the absolute value of A is not known. The response $\Delta V_{1,2}$ was obtained when both electrodes were pulsed simultaneously (i.e. response to twice A). By successively matching responses, a complete dose–response curve can be generated, from which a Hill coefficient can be derived. The two ACh electrode procedure makes no assumptions about the zero point of ACh release or linearity of the ACh electrodes.

α-Bungarotoxin purification and iodination

BTX was purified by gel filtration from crude snake venom (Sigma or Miami Serpentarium) according to the method of Chang & Lee (1963). The purified toxin was iodinated by the lactoperoxidase method of David (1972) to yield about 0·1 I atom per BTX molecule. The unreacted ^{125}I and the lactoperoxidase were separated from the toxin by G-50 gel filtration. The fractions from the G-50 column were assayed for protein by absorption of 280 nm light and for ^{125}I by scintillation counting. A small lactoperoxidase peak was followed by the large BTX peak located about a factor of 2 in volume after the void volume. For unknown reasons, the fraction with peak radioactivity and that with peak protein were not coincident. Binding activity of the radioactive fractions was tested on lyophilized *Torpedo marmorata* electroplax by studying the competition of [^{125}I]BTX with cold BTX. Occasionally a fraction which showed the highest specific activity did not competitively inhibit binding of cold toxin. Labelled BTX fractions were used only when cold toxin competitively inhibited labelled toxin binding. The specific activity of the [^{125}I]BTX determined by competition agreed within 20 % of the value obtained using absorbance at 280 nm and scintillation counting. The specific activities used to convert grain densities to BTX site densities were the values obtained by competition binding. The values ranged from 60 to 120 c/m-mole.

The inactivation rate of myotube AChR by [^{125}I]BTX was measured for each new batch of [^{125}I]BTX to assess its reproducibility. After obtaining control ACh sensitivity, a single myotube was impaled for 30–180 min in the presence of 10^{-7} M [^{125}I]BTX, the concentration used throughout this paper. ACh dose–response curves were taken every 5–10 min and from these curves the [^{125}I]BTX binding rate could be derived. Controls to which no BTX was added gave constant shaped dose–response curves for up to 90 min.

Determination of α-BTX site density by light autoradiography

[^{125}I]BTX binding site density was determined by light microscope autoradiography. Myotubes in Tyrode were treated with [^{125}I]α-BTX (10^{-7} M) for 1 hr, long enough to inactivate greater than 98 % of the ACh response. The myotubes were then washed in Tyrode plus bovine serum albumin, 2 mg/ml., for 1·5 hr with three changes of medium. Glutaraldehyde (2 %) fixation in 53 mM-Na_2HPO_4 and 13 mM-KH_2PO_4 buffer for 30 min followed the washing. The myotubes were then rinsed in the above buffer plus 0·2 M sucrose (three changes 5 min apart), water rinsed, and air dried. All manipulations were carried out at 19–21° C and pH = 7·4.

To ensure a uniform emulsion coating over the dried cells, a monolayer stripping film procedure was devised and calibrated for sensitivity to ^{125}I. A monolayer of

emulsion was formed on a collodion coated slide comparable to that used in the flat substrate electron microscopic autoradiographic procedure of Salpeter & Bachmann (1964, 1972). A deep purple interference colour was used as a criterion for the desired emulsion thickness and uniformity. In the darkroom, under Wratten AO safe-light filter (yellow-green), the collodion plus emulsion of desired thickness was stripped on to a distilled water surface using 10% HF as a stripping aid (see Salpeter & Bachmann, 1972). The film was then lifted from below on to a square of filter paper (Whatman no. 50) from which a small hole had been cut, and was placed emulsion side down over the cells. Circles scratched on the bottom of the tissue culture dishes marked groups of cells upon which electrophysiology had been done. The filter paper was allowed to dry down on the cells for about 2–3 min, and the tissue culture dish was then dipped into a dish containing water and inverted, causing the filter paper to imbibe water and fall off, leaving the emulsion layer adhering to the cells. Occasionally the emulsion layer did not lie smoothly to the cells. This could be determined visually while holding the dish up to the safe-light, and if necessary the emulsion could be washed off and replaced.

Using the above procedure the emulsion is directly in contact with the cells and the collodion backing is on the other side of the emulsion. This is advantageous since the low emergy electrons ($\sim$ 3–4 keV) emitted by the ^{125}I do not have to traverse the backing layer before reaching the emulsion. This avoids absorption and scattering within the backing layer which could cause fluctuations in sensitivity and problems with calibration. However, the close proximity of emulsion to cells causes a risk of chemography (the test for chemography is described below). Furthermore, before the emulsion is developed, the collodion film has to be removed. This is done by a 5 min wash in 100% ethanol followed by a few ethanol rinsed and then air drying. The emulsion is then developed with D-19 (Kodak) at room temperature for 4 min, rinsed in distilled water and then fixed with non-hardening fixed (Gevaert) for 2 min and finally rinsed in water and air dried.

The emulsion was calibrated for sensitivity as follows. A 0·8% aqueous solution of ^{125}I albumin was dropped on to a glass slide, drained and allowed to dry. The resultant thin film of albumin was fixed in paraformaldehyde vapour, washed and scored into small squares. The squares were stripped on to water, using 10% HF as a stripping aid. Individual squares were picked up on to tissue culture dishes and their thickness measured using an incident light Nomarski interferometer (attachment to the Reichert Zetopan light microscope). Films were used as test specimens if they had an average thickness of less than 800 Å and if all four corners were within 10% of the mean thickness. This thickness was chosen since self absorption is not a significant factor even with the low energy ^{125}I electrons (Fertuck & Salpeter, 1974). The squares which had a known specific activity were then coated with emulsion as described above, exposed for 4–7 days and developed, as for the tissue culture cells. Developed grains were counted per unit area of emulsion using a calibrated ocular, 2500×, phase-contrast microscope. The emulsion efficiency (grains/nuclear events) was calculated from the specific activity of the albumin and found to be $0{\cdot}56 \pm 0{\cdot}03$. (Since this study was initiated the supplier of Ilford L4 emulsion has changed from Ilford Co., Ltd, England to Polysciences, U.S.A. We have found a decrease in sensitivity by about 25%.) As one might expect, this sensitivity for the light microscope technique using a thin source and a monolayer Ilford L4 emulsion was the same as was previously obtained for the electron microscopic autoradiographic procedure under similar specimen conditions (Fertuck & Salpeter, 1974). A different calibration would hold for thick sources and for thick emulsion due to absorption of low energy electrons and detection of high energy γ-rays.

The calibration for chemography (i.e. effect on sensitivity due to chemical

interaction with cells) involved exposing the emulsion simultaneously to an independent ^{125}I source and non-radioactive fixed tissue. Non-radioactive tissue culture cells fixed in 2% glutaraldehyde were coated with emulsion as described above. The backing collodion was removed by 100% ethanol and a cover slide containing an [^{125}I]albumin square of measured thickness was pressed on top of the emulsion. The emulsion layer was thus sandwiched between tissue on one side and a radioactive source on the other. After exposure, the cover glass with albumin film was removed and the emulsion developed. The number of grains per unit area over cells was compared to that over the dish devoid of cells. Sparsely cultured cells were used so that large regions of dish without cells were available. We found the sensitivity over cells to be somewhat more variable especially if OsO_4 was included in the fixation and occasionally lower than over the dish. This negative chemography was eliminated if a thin (50–70 Å) layer of carbon was evaporated over the cells before coating with emulsion. All our autoradiographic experiments were therefore performed with carbon coated cells.

Individual myotubes on which physiological measurements were done could be recognized by their morphology within marked circles on the tissue culture dish. Silver grains over myotubes were counted using a calibrated ocular 2500×, phase-contrast microscope. Counting was done over the myotubes within 30 μm of the ACh iontophoresis site (this distance was chosen because it was sure to include the area covered by the ACh pulses). For each exposure time in days (t_e), BTX storage time in days (t_s), grain density per μm^2 (G), inverse efficiency (d), and specific activity at zero storage time in c/m-mole (A_0), the number of sites per μm^2 (S) is given by from Fertuck & Salpeter, 1974)

$$S = \frac{2{\cdot}17 \times 10^3 (G)d}{A_0(1 - e^{-0{\cdot}01155 t_e} e^{-0{\cdot}01155 t_s})}. \quad (4)$$

Surface topography of the myotubes

To determine whether the surface morphology of the myotubes was sufficiently flat to give accurate values for membrane area, culture dishes containing L6 myotubes were examined by scanning electron microscopy. Cells grown on tissue culture dishes were fixed in 2% glutaraldehyde + 0·1% OsO_4 as for transmission electron microscopy. While the dishes were immersed in buffer, small chips of the dish were cut out and these were then dehydrated and critical point dried in freon according to the methods of Miller & Revel (1975). The chips were then mounted on metal specimen disks, rotary shadowed with gold and examined with an ETEC scanning electron microscope.

Electron microscope autoradiography

Cells were fixed for electron microscopy in 2% glutaraldehyde + 0·1% OsO_4 in 0·1 M phosphate buffer for 5–10 min at room temperature and then in 2% glutaraldehyde for 30 min at 4° C. The addition of OsO_4 produced a more consistent fixation than glutaraldehyde alone. The cells were then rinsed for 1 hr in several changes of 0·25 M sucrose + 0·1 M phosphate buffer at 4° C, post-fixed in 1% OsO_4, stained with 2% aqueous uranyl acetate and dehydrated in graded ethanol. A thin layer of Epon 812 was then polymerized in the dish. Individual cells were identified within the Epon and their location marked. Small squares containing the cells, the plastic dish and Epon layer were sawed out using a thin saw wire. The Epon containing the cells was separated from the dish and was reimbedded in Epon using a flat embedding boat. Silver to pale gold sections were cut on a Huxley microtome and examined with a Philips 201 or 300 electron microscope. Pale gold sections were

mounted for electron microscope autoradiography according to the 'flat substrate' procedure of Salpeter & Bachmann (1964, 1972). Sections were cut from several levels of the same myotube. Monolayers of Ilford L4 emulsion were used and developed with a gold latensification-EAS developer as calibrated by Salpeter & Bachmann (1972). Electron microscope grids containing electron microscopic autoradiographs from different regions of each myotube were fully photographed, wherever an image of a myotube was present, independent of the number of grains on the picture. The total length of plasma membrane and the total area of internal cytoplasm represented in these pictures was obtained using a calibrated grid method as previously described (Fertuck & Salpeter, 1976). To determine a grain density related to plasma membrane we counted developed grains up to 3000 Å either side of the membrane (this constitutes > 3·5 resolution distances, which was shown by M. M. Salpeter *et al.* (in the press) to contain more than 90 % of developed grains expected from an iodinated line source). Grains per equal area of autoradiogram over myotube cytoplasm (at a distance beyond radiation spread from the plasma membrane) was considered cytoplasmic label and was subtracted to give a membrane related label. Since the thickness of the sections was measured by interferometry, grain density (G) could be expressed per μm^2 of membrane surface or per μm^3 of cytoplasm. Eqn. (1) was then used to calculate α-BTX site density for both membrane area and tissue volume as had been done from the light microscope autoradiographically derived grain densities.

Basic premises

When ACh is released from a pipette it will cover a certain area, a, of the myotube and this area depends on the distance of the electrode from the myotube and on the concentration of the ACh, A. Since the conductance is the summed response of all open channels (Katz & Miledi, 1972; Anderson & Stevens, 1973) then, if there were no interaction between adjacent AChR. complexes,

$$\left.\begin{aligned} g &\equiv Gf(A_p) = a_p\sigma\gamma f(A_p); \\ G &\equiv a_p\sigma\gamma \end{aligned}\right\}, \tag{5}$$

where G is the response at infinite concentration, a_p is the area over which ACh has diffused at time, t_p, of peak response, A_p is the ACh concentration A over the area at this time, γ is the conductance per open channel and σ is the AChR site density. In this relation $f(A_p)$ is the dose–response function or the fraction of total channels which are open by concentration A_p (i.e. the ratio of channels opened by concentration A_p to that which would be opened at infinite saturating concentration). The dose–response function $f(A)$ we used is the Hill relation which in simplified form can be written as

$$f(A) = \frac{A^n}{A_0^n + A^n}, \tag{6}$$

where A_0 is an apparent dissociation constant (or the concentration at which half the maximum number of channels are open) and n is the Hill coefficient.

Finally we should bear in mind the different consequences if the ACh concentration delivered to the myotube is non-saturating $A \ll A_0$ or saturating $A \gg A_0$. First let us consider the condition of non-saturating ACh concentrations or $A \ll A_0$. From the Hill relation, eqn. (6), we see that under these conditions $f(A) \propto A^n$. A, the concentration over the membrane area a, is proportional to Q/a^1 (or Q/volume) provided one has established, as will be seen later, that Q is linear with dose A. Thus from eqn. (5) membrane response $g \propto a_p A^n \propto a_p Q^n/a^{3n/2}$. If $n > 2/3$, the membrane response then decreases with increasing area. It follows that under non-saturating conditions the response peaks at the smallest area seen by the ACh pulse. The time to peak t_p

will then be independent of Q and so will the area a_p covered at peak response. Thus from eqn. (5) we get that for non-saturating ACh

$$g \propto GQ^n \propto \sigma Q^n. \tag{7}$$

For saturating ACh concentrations or $A \gg A_0$, we get from eqn. (6) that $f(A) \simeq 1$. Then it can be seen from eqn. (5) that the membrane response (g) which is $\sim \sigma a f(A)$ increases with area until $A_p \sim A_0$. The peak response g is then reached at area a_p where $cQ/a_p^{\frac{1}{2}} = A_0$ (with c and A_0 being constants, and $a_p \propto Q^{\frac{2}{3}}$). Thus for saturating ACh we get

$$g \propto \sigma a_p \propto \sigma Q^{\frac{2}{3}}. \tag{8}$$

Thus eqn. (8) for saturating ACh concentration has the same form as eqn. (7) but $n = 2/3$ instead of being the Hill coefficient.

RESULTS

Response characteristics of myotubes to applied ACh

An example of depolarization as a function of time is given in Fig. 1*A*, and of ΔV as a function of Q is given in Fig. 1*B*. (The time-to-peak t_p was 20–50 msec for electrode to myotube distances of 1·4 μm and was independent of ACh dose.) The input resistance R_{in} measured as illustrated in Fig. 1*C* varied from 3 to 45 MΩ at 5–10 mV depolarization (6 MΩ for sample given in Text-fig. 1*C*). The range of values for the resting potential E_m was 38–58 mV on L6 and 40–50 mV on primary myotubes. Sensitivity, in mV/nC, which we will call voltage sensitivity, S_v, was computed for comparison with other work in which voltage sensitivity is the index used. For this measure we used the average slope of the $\Delta V(Q)$ curve, $\mathrm{d}(\Delta V)/\mathrm{d}Q$, in the ΔV range of $\sim$ 10 mV.

We obtained S_v values ranging from 20 to 1600 mV/nC for L6 myotubes and from 400–1600 mV/nC for rat primary myotubes. As stated in the Methods we chose to use a measure for sensitivity which is independent of membrane potential and input resistance. This value is $S_g = g/Q^n$, with g derived from eqn. (2). To justify this formulation we must consider the Hill relation given in eqn. (6). We do not have a direct measure of A but using the two-electrode method of Katz & Thesleff (1957) described in Methods we obtained a ratio scale for ACh dose (Text-fig. 2). It can be seen that above the holding current the ACh dose (A) is linear with the iontophoretic charge Q over a tenfold range.

The two-electrode experiment also allowed us to generate a dose–response curve by plotting $V_{1,2}$ (the response to twice a given dose A) *vs.* $V_1 + V_2$ (twice the response to that dose). Such a plot is given in Text-fig. 3*A*. From Text-fig. 3*A* we see that at low levels of depolarization the response to $2A$, $V_{1,2}$, is higher than would be expected from a simple addition of $2V_1$. As pointed out by Katz & Thesleff (1957) and Hartzell *et al.*

(1975), such a potentiation is expected if the ACh dose–response curve is sigmoid (Hill coefficient > 1).

To obtain a Hill coefficient from our double electrode data we used eqns. (5) and (6) to derive a relation between g_{12} and $2g_1$, i.e. the con-

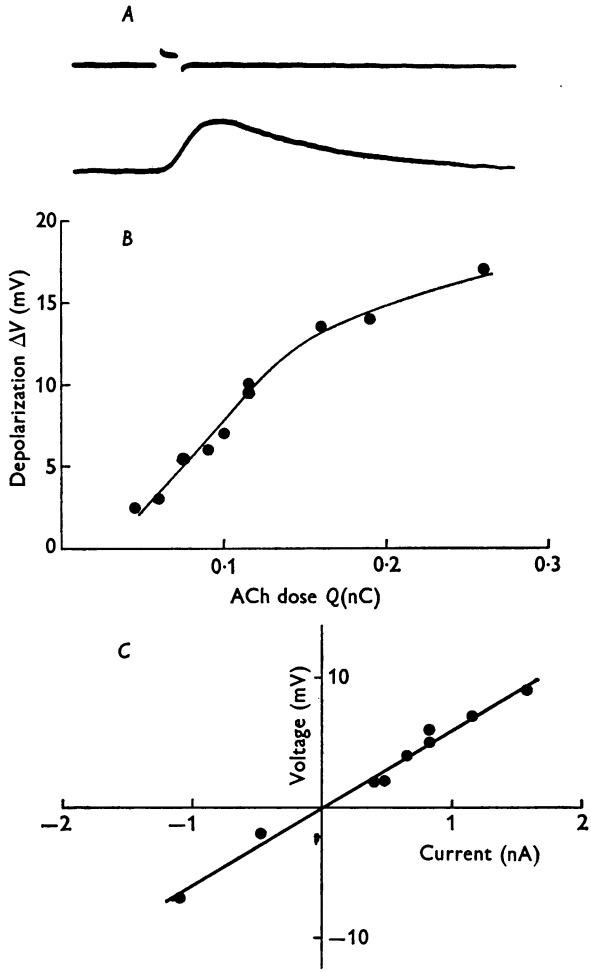

Text-fig. 1. *A*, Time course of ACh induced depolarization. The top trace is the ACh electrode current record. The release pulse is 0·05 nC in amplitude and 10 msec long. The bottom trace displays the resulting depolarization of 2 mV from an E_m of 50 mV. Peak depolarization ΔV is used in Fig. 1*B* to give a dose–response curve. *B*, ACh depolarization ΔV plotted against ACh dose Q. *C*, current–voltage relation for a myotube. A fixed current was intracellularly applied and the resulting steady-state voltage read. The slope of the line yields the input resistance.

ductances corresponding to the responses V_{12} and $2V_1$. This relation can be written as

$$\frac{1}{g_{12}} = \frac{2^n - 1}{2^n}\frac{1}{G} + \frac{1}{2^{n-1}}\frac{1}{2g_1}, \tag{9}$$

where $G = a_p \sigma \gamma$ (eqn. (5)), or the maximum conductance change possible over area a_p. A plot of $1/g_{12}$ against $1/2g_1$ should result in a straight line of slope 2^{1-n} (with an intercept related to $1/G$). Our double electrode dose–response curve was replotted in this form. One example is shown in Text-fig. 3*B*. This plot approximates a straight line, justifying the Hill assumption in eqn. (6), and the Hill coefficient n can be derived from its slope ($n \approx 1{\cdot}7$ for the example in Fig. 3*B*). In principle, according to eqn. (9), the intercept in such a plot yields $1/G$. For our experimental conditions, we merely found that $g/G \ll 1$, and cannot be distinguished from zero, or in other words, our experimental conditions were far from 'conductance saturation'.

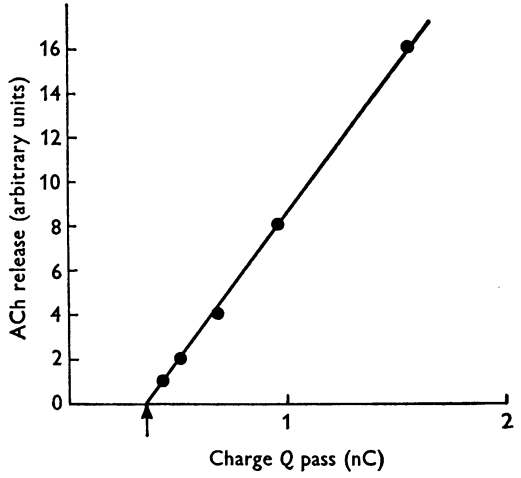

Text-fig. 2. Computed ACh release as a function of charge passed from the iontophoretic electrode. As described in the text, the application of ACh from two electrodes allows one to obtain the shape of the electrode release function as well as the shape of the myotube response function. The ACh release was linear with charge passage and extrapolated to zero approximately at the value of charge which just balanced the holding current.

Values of n were obtained in six preparations. To ensure that the same general area of the myotube was intersected by ACh from both electrodes, the electrodes were placed $> 6\,\mu$m from the myotube, which was considerably greater than the spacing between the electrodes. Under these conditions we obtained values of $n \simeq 1{\cdot}7 \pm 0{\cdot}2$.

These data show that under our experimental conditions $g \propto Q^n$ with $n \approx 1{\cdot}7$ and thus our definition of sensitivity $S_g \equiv g/Q^n$ is independent of Q. Thus if there is no interaction between adjacent AChR complexes, eqns. (5) and (7) should hold, and S_g for different myotubes should simply

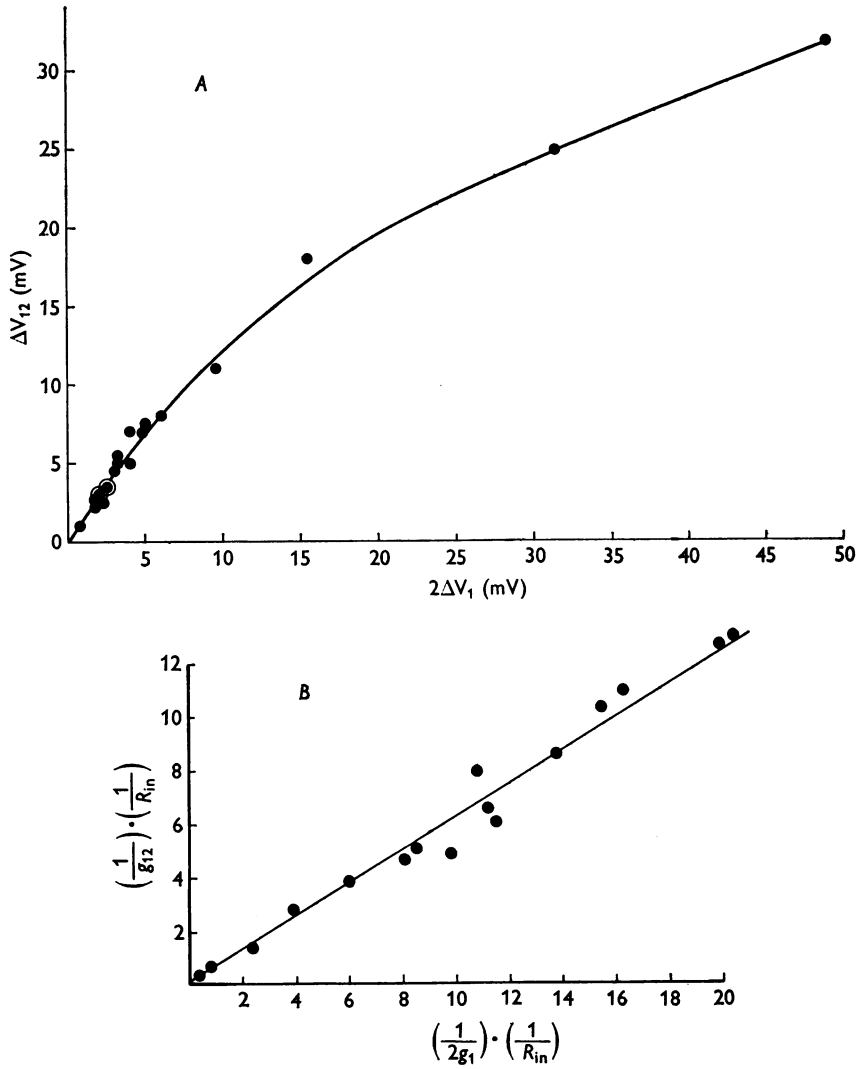

Text-fig. 3. *A*, two electrode response curve. Twice the single electrode response ΔV_1 is plotted against ΔV_{12}, the response obtained when both electrodes were pulsed simultaneously. *B*, plot of $1/g_{12}$ *vs.* $1/2\,g_1$, obtained from ΔV_{12} and $2\Delta V_1$ using eqn. (2). For this myotube the input resistance R_{in} was not known, and thus the conductances are in units of $1/R_{in}$. This however does not affect the slope determination.

be proportional to AChR site density σ. Text-fig. 4*A–C* give experimental samples of log g *vs.* log Q, fitted to a line of slope 1·7 to obtain a single value for sensitivity (S_g) for each myotube as described in Methods.

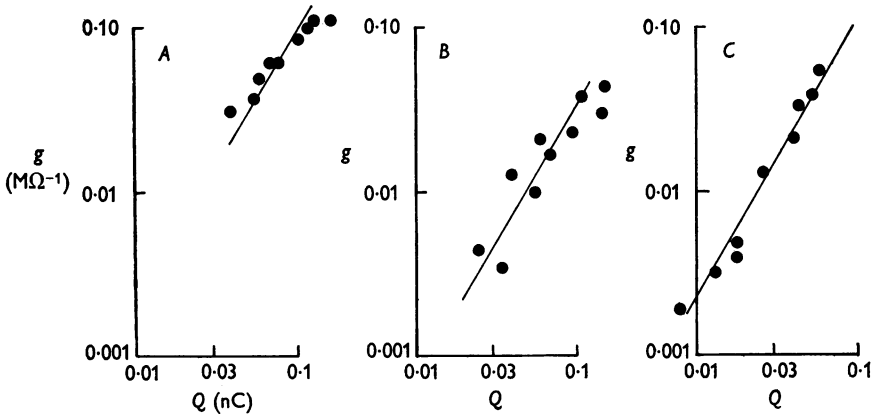

Text-fig. 4. Range of plots of log g *vs.* log Q used to obtain a sensitivity index. The intercepts on the axis corresponding to 0·01 nC were used as the measure of sensitivity. These plots assume $g = KQ^{1·7}$ and the intercept is proportional to K.

Acetylcholine receptor site density (σ)

A measurement of [^{125}I]α-BTX binding rate was necessary to determine how long α-BTX should be applied to saturate the receptors. Text-fig. 5 is a semilog plot showing the time course of [^{125}I]α-BTX inactivation of the conductance g, obtained from eqn. (2), for a single L6 myotube at five ACh doses. Note that all five curves in Text-fig. 5 are straight lines with almost the same slope, thereby showing that conductance (g) decays exponentially with time in BTX with a half-time independent of ACh dose. The half-time varied for different cells from 4 to 7 min with a mean and S.E. of 5·4 ± 0·5 min. Myotubes from primary and L6 cultures showed no significant difference in α-BTX binding rate. With such a short half-time of inactivation it is clear that one hour in BTX at 10^{-7} M is a long enough time to block essentially all AChR.

Pl. 1*A*, *B* and *C* show typical light autoradiographs of L6 and primary myotubes. The grains on L6 myotubes appear to be evenly distributed over the entire surface with no clumping, while primary cultures frequently show variations in grain density with occasional clumps of very high grain density, or 'hot spots'. A linear array or streaking of grains was frequently seen in both types of myotubes. To quantify the general impression of grain distributions, grain counts were made per calibrated grid area (11·3 μm^2) along a region 60 μm long centred at the site at which the ACh

sensitivity was determined. The number of grains per calibrated grid area was plotted in histogram form (Text-fig. 6*A* and *B*) and compared with a Poisson distribution. We found a Poisson distribution of the developed grains on all L6 myotubes tested, but not for the grain distributions on

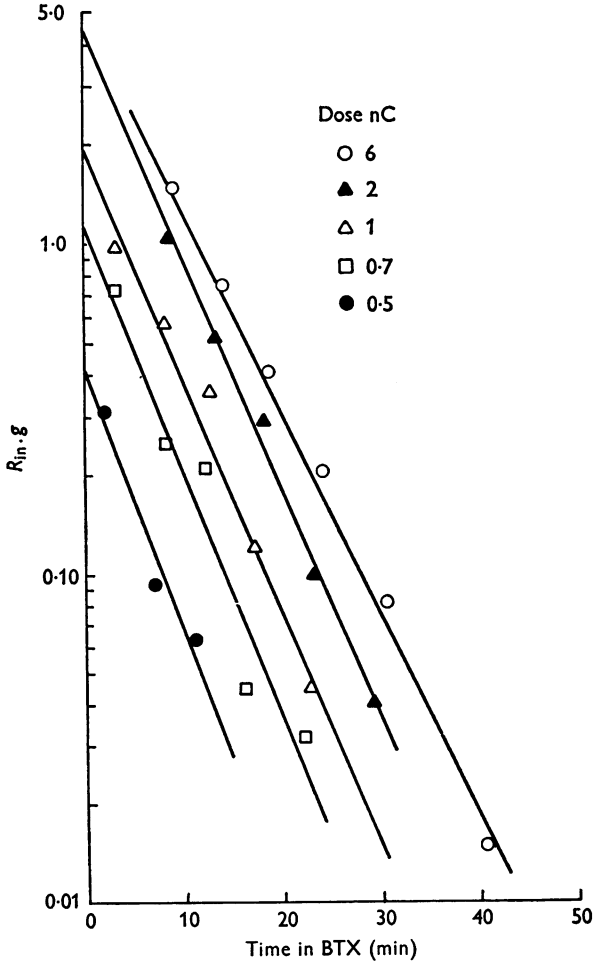

Text-fig. 5. A semilog plot of conductance, *g*, *vs.* time in α-BTX. The five lines are at five different doses of ACh. The poisoning appeared first order with a half-time of 4·3 min for this myotube.

primary myotubes. This establishes that the α-BTX binding sites are uniformly distributed on L6 but are distributed with non-uniform density over the surface of primary myotubes.

Myoblast labelling by [^{125}I]BTX was less than twice the dish background. Our physiological measurement of ACh sensitivity using ~ 100 times the

ACh dose needed to depolarize myotubes yielded no detectable response and this is consistent with the low level ($\leqslant$ 6 sites/μm^2) of α-BTX density measured. Myoblast labelling was therefore considered non-specific and was subtracted from counts over myotubes. Labelling on myotubes was 2–80 times the labelling on myoblasts.

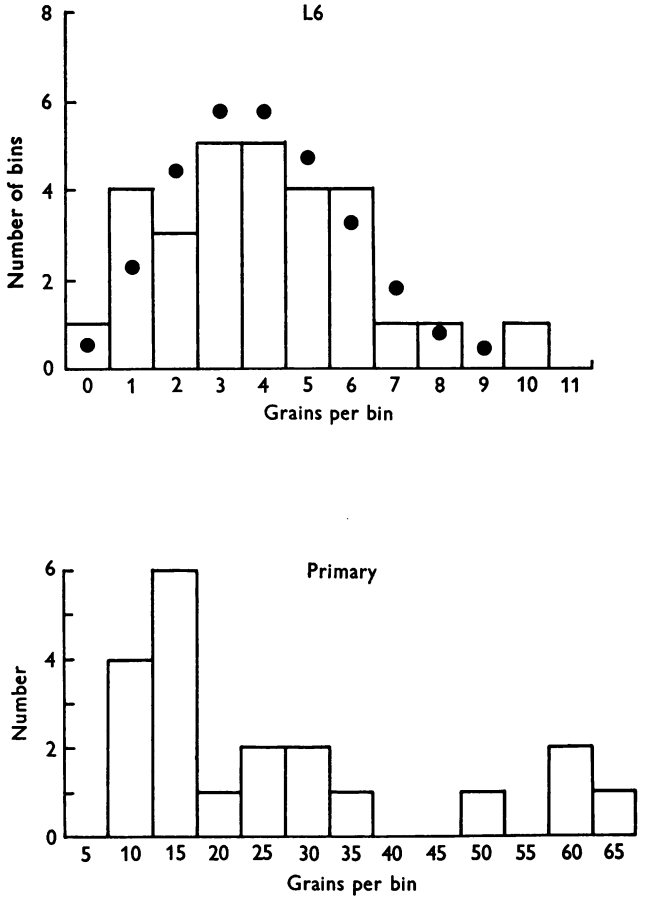

Text-fig. 6. Histograms of autoradiographic grain distributions on the surface of L6 and primary myotubes. Circles over the L6 data are the computed Poisson values with the same mean as the observed distribution (χ^2 = 3·55, d.f. = 6, $P > 0{\cdot}5$). The primary myotube grain densities did not fit any simple distribution, implying spatial gradients on the myotube.

Average α-BTX site densities were calculated from average grain counts per calibrated grid area using eqn. (4). Values of average site density from 5 to 400 per μm^2 were obtained on L6 myotubes (with most between 15 and 200) and from 54 to 900 per μm^2 on primary myotubes (with most

between 200 and 600). However, 'hot spots' ($\sim 20\,\mu m^2$ in diameter) which were occasionally seen on primary myotubes (see Pl. 1) contained localized BTX site densities as high as 3000–4000 sites/μm^2. No 'hot spots' were encountered within the area tabulated for the correlation between α-BTX binding and ACh sensitivity.

Pl. 1*D* gives a surface view by scanning electron microscope of a L6 myotube. We see that the myotube is quite flat and smooth indicating that the surface area measured by light microscopy was a close approximation to the true membrane area. The surface of mononucleated cells frequently showed villi and ruffles indicating that the flat surface of the myotube was not a result of inadequate technical preparation. Transmission micrographs confirm this conclusion.

To find if our α-BTX label was restricted to the plasma membrane, electron microscope autoradiography was carried out on seven primary rat myotubes (the average site density on the L6 was too low for efficient electron microscope autoradiographic study). For two of these myotubes autoradiograms were prepared from semi-serial sections and a sufficiently large number of grains ($\sim$ 350 grains per myotube) was obtained to give statistically reliable site densities specific for each myotube. The data from the remaining five myotubes were pooled. Pl. 2 illustrates one such autoradiogram. We found that $\sim 70\%$ of the developed grains appeared within 3000 Å of the plasma membrane (i.e. $\sim$ 3·5 HD from the membrane, a distance which would contain 90% of all grains due to an ^{125}I line source; M. M. Salpeter *et al.* 1977). These grains could therefore have been derived by radiation spread from the membrane. A residual 25–30% of the total grains are beyond that distance and are thus due to radioactivity not localized on the surface. Because of the short range of the low energy electron emitted by ^{125}I and the low sensivity of the monolayer L4 emulsion to the higher energy γ-rays emitted by ^{125}I (Fertuck & Salpeter, 1974), virtually no grains from the internalized label would appear in the light autoradiography. Internal grains do not seem to be associated with any specific organelles.

The site density calculated from the electron microscope autoradiograms using eqn. (4) gave about thirty sites per μm^3 of internal myotube cytoplasm and $\sim$ 116–260 sites/μm^2 of plasma membrane. These membrane values are within the range of those obtained by light autoradiography. If the thickness of a membrane is $\sim$ 100 Å, then per volume of tissue the membrane label (18,800 sites/μm_3) is $\sim$ 600 times higher than the internal cytoplasmic label.

On some cells there was a significantly (two to threefold) higher α-BTX site density on the part of the plasma membrane which was in contact with the tissue culture dish (Pl. 2). Areas of myotube in contact with other

cells did not have the same higher site density as did those areas in contact with the culture dish. We have no explanation for this observation, except to speculate that it may reflect some membrane flow phenomena, or that the dish is a stimulant to differentiation. Since the light autoradiography and ACh pulses both see only the top surface of the cells, only the top surface values are at present relevant to our study.

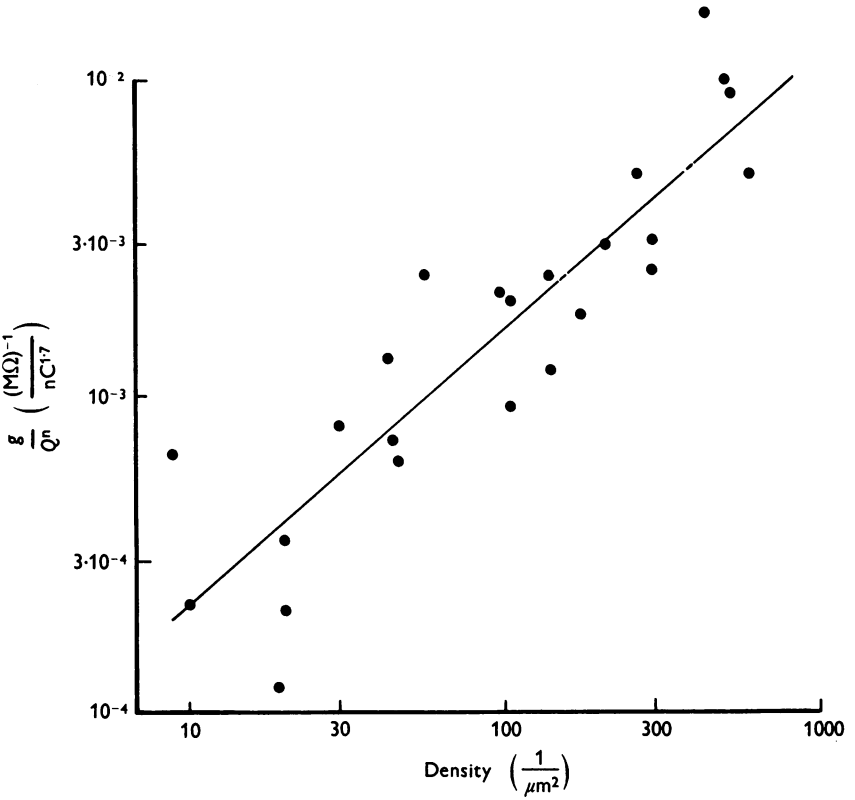

Text-fig. 7. A log–log plot of ACh sensitivity, S_g versus AChR site density (σ), for different myotubes. The slope of the least-squares line is $0{\cdot}9 \pm 0{\cdot}2$.

The correlation between conductance sensitivities S_g and AChR site densities σ for the same myotubes is shown in Text-fig. 7. The regression of conductance sensitivity upon density yielded a slope of $0{\cdot}9 \pm 0{\cdot}2$ (the error reflects the uncertainty in the value of n and the scatter of the points of Fig. 7). This result confirms that S_g is proportional to σ.

DISCUSSION

In the present study we obtained a correlation between AChR site density and ACh sensitivity. When site density (σ) is plotted against conductance sensitivity $S_g \equiv (g/Q^n)$ on a log–log plot (with n being the

experimentally obtained Hill coefficient = 1·7) we get a linear relationship with a slope of 0·9 ± 0·2 or essentially unity. This relationship verifies that our data are compatible with n, $f(A)$ and γ being independent of σ and confirms the validity of eqns. (5), (6) and (7) for our system.

In order to compare the results obtained by us with those of others, it should be pointed out that the slope of the relationship between sensitivity and site density depends both on the definition of sensitivity and on the experimental conditions under which sensitivity is obtained. If as some have done, sensitivity is defined as $\Delta V/Q$ then as shown in eqns. (1) and (2) the response itself is dependent on the input resistance and membrane potential. In addition even if a value for g is calculated to correct for R_{in} and E_{m} and sensitivity defined as g/Q then due to the non-linear dose–response characteristics the value of g/Q is not a constant for a given cell but depends on which part of the dose–response curve the data is obtained. Different sensitivity values are then comparable only if the dose Q is kept constant during the experiment and between experiments. The problem can be eliminated if the dose–response characteristics are included in the definition of sensitivity as we have done by using $S_g = g/Q^n$. Even here one should note that n is the Hill coefficient only if the experiment is performed under non-saturating conditions of ACh as shown by comparing eqns. (7) and (8).

In this context it is of interest to compare our results with those of Hartzell & Fambrough (1972), who obtained a relationship between ACh sensitivity ($\Delta V/Q$) versus AChR site density (σ) approaching the form $\Delta V \propto \sigma Q^2_3$ whereas in our study we get $\Delta V \propto \sigma Q^{1\cdot7}$. From eqns. (7) and (8) we see that the relation obtained by Hartzell & Fambrough would exist under saturating ACh conditions whereas ours would exist under non-saturating conditions. We have indeed shown from Text-fig. 3*B* that our experimental conditions were far from saturation, but we do not have enough information to test whether the experimental conditions used by Hartzell & Fambrough were indeed saturating.

The AChR site densities on L6 myotubes ranged from 5 to 400 sites/μm^2 and on rat myotubes from 54 to 900 sites/μm^2 (excluding hot spots). Our rat primary values are considerably lower than the 1500–2000 sites/μm^2 reported by Hartzell & Fambrough (1973) for such cells. However, Hartzell & Fambrough did not calibrate their autoradiographic conditions but adopted the calibration of Ada, Humphrey, Askonas, McDevitt & Nossal (1966) which may not have been valid for their experimental conditions. It has been noted that the distribution of AChR sites varies with the developmental age of chick primary myotubes, being more uniform on younger myotubes and displaying hot spots with age (Sytkowski, Vogel & Nirenberg, 1973). We found a deviation from Poisson statistics to be

evident in rat primary myotubes ranging in age from 4 to 14 days after plating. L6 myotubes remained uniform over this age scale.

It has been reported that functional synaptic connexions can be made on L6 myotubes (Kidokoro & Heinemann, 1974). In view of the uniform distribution of α-BTX binding on L6 myotubes these experiments suggest that preformed 'hot spots' appear not to be a prerequisite for the formation of neuromuscular junctions

Our electron microscope autoradiographic studies have also indicated the presence of an internal cytoplasmic label, unique to myotubes (i.e. not present in myoblasts) and present in a relatively constant quantitative relationship with the surface label ($\sim$ 30% of total label). This internal label is present at the earliest time studied, i.e. at the end of the 1 hr incubation period plus 1 hr wash at room temperature and thus under conditions where internalization of surface label for the purpose of degradation has been reported not to be taking place (Devroetes & Fambrough, 1975). The significance of this myotube specific label is unclear.

The linear relation between sensitivity and site density over a range of 10–600 sites/μm^2 of the form given in eqn. (7)

$$g \propto \sigma Q^n$$

indicates that no interaction was occurring between adjacent ion channels of AChR complexes. It also indicates that in myotubes, the development of ACh binding sites does not precede its coupling with functional ion channels, and that the two entities of a functional AChR complex, i.e. AChRs and channels, are from the beginning seen in the same quantitative ratio with each other. Furthermore, it indicates that at least for this developmental system higher ACh sensitivity does not reflect increased responsiveness of individual AChR complexes but merely reflects increased AChR site density.

Finally the Hill coefficient, $n = 1{\cdot}7$, obtained from our studies using the double electrode procedure was independent of AChR site density and is in line with the values ranging from 1·6 to 2·2 obtained from various adult systems (Hartzell *et al.* 1975; Changeux & Podleski, 1968; Feltz & Mallart, 1971; Katz & Thesleff, 1957). One exception is the value of $n = 3$ measured on frog by Dreyer & Peper (1975). Thus, even though the highest AChR density on myotubes is some hundredfold below the AChR density at adult end-plates, the Hill coefficient is about the same. Therefore if a Hill coefficient greater than unity reflects positive co-operativity, this co-operativity must be independent of average AChR complex density and can only reflect interactions between AChR subunits within an AChR complex.

We thank Julie Matthews-Bellinger, Ralph Loring, and Peter Ravdin for preparation and characterization of the [^{125}I]bungarotoxin, and Mary Johnson and Susan Nichols for technical assistance. Supported by Grants NS 09315, GM 10422 and NS 10638 from the National Institutes of Health, Bethesda, Ind., U.S.A.

REFERENCES

ADA, G. L., HUMPHREY, J. H., ASKONAS, B. A., MCDEVITT, H. O. & NOSSAL, G. J. V. (1966). Correlation of grain counts with radioactivity (^{125}I and tritium) in autoradiography. *Expl Cell Res.* **41**, 557.

ANDERSON, C. R. & STEVENS, C. F. (1973). Voltage clamp analysis of acetylcholine produced end-plate current fluctuations at frog neuromuscular junction. *J. Physiol.* **235**, 655–691.

AXELSSON, A. & THESLEFF, S. (1959). A study of supersensitivity in denervated mammalian skeletal muscle. *J. Physiol.* **147**, 178–193.

BARNARD, E. A., DOLLY, J. O., PORTER, C. & ALBUQUERQUE, E. (1975). The acetylcholine receptor and the ionic conductance modulation system of skeletal muscle. *Expl Neurol.* **48**, 1–28.

BARNARD, E. A., WIECKOWSKI, J. & CHIU, T. H. (1971). Cholinergic receptor molecules and cholinesterase molecules at mouse skeletal muscle junctions. *Nature, Lond.* **234**, 207–209.

BRENNECKE, R. & LINDEMANN, B. (1971). A chopped-current clamp for current injection and recording of membrane polarization with single electrodes of changing resitance. *T.I.T. J. Life Sci.* **1**, 53–58.

CHANG, C. C. & LEE, C. Y. (1963). Isolation of neurotoxins from the venom of *Bungarus multicintus* and their modes of neuromuscular blocking action. *Archs int. Pharmacodyn. Thér.* **144**, 241–257.

CHANGEUX, J.-P. & PODLESKI, T. R. (1968). On the excitability and cooperativity of the electroplax membrane. *Proc. natn. Acad. Sci. U.S.A.* **59**, 944–950.

CHANGEUX, J.-P., THIERY, J., TUNG, Y. & KITTEL, C. (1967). On the cooperativity of biological membranes. *Proc. natn. Acad. Sci. U.S.A.* **57**, 335–341.

DAVID, G. S. (1972). Solid state lactoperoxidase: a highly stable enzyme for simple, gentle iodination of proteins. *Biochem. biophys. Res. Commun.* **48**, 464–471.

DIAMOND, J. & MILEDI, R. (1962). A study of foetal and new-born rat muscle fibres. *J. Physiol.* **162**, 393–408.

DEVROETES, P. N. & FAMBROUGH, D. M. (1975). Acetylcholine receptor turnover in membranes of developing muscle fibres. *J. cell Biol.* **65**, 335–358.

DREYER, F. & PEPER, K. (1974). Iontophoretic application of acetylcholine: advantages of high resistance micropipets in connection with an electronic current pump. *Pflügers Arch. ges. Physiol.* **348**, 263–272.

DREYER, F. & PEPER, K. (1975). Density and dose–response curve of acetylcholine receptors in frog neuromuscular junctions. *Nature, Lond.* **253**, 641–643.

FATT, P. & KATZ, B. (1951). An analysis of the end-plate potential recorded with an intracellular electrode. *J. Physiol.* **115**, 320–370.

FELTZ, A. & MALLART, A. (1971). An analysis of acetylcholine responses of junctional and extrajunctional receptors of frog muscle fibres. *J. Physiol.* **218**, 85–100.

FERTUCK, H. C. & SALTPETER, M. M. (1974). Sensitivity in EM autoradiography for ^{125}I. *J. Histochem. Cytochem.* **22**, 80–87.

FERTUCK, H. C. & SALPETER, M. M. (1976). Quantitation of junctional and extrajunctional acetylcholine receptors by electron microscope autoradiography after ^{125}I-α-Bungarotoxin binding at mouse neuromuscular junctions. *J. cell Biol.* **69**, 144–158.

FISCHBACH, G. D. & COHEN, S. A. (1973). The distribution of acetylcholine sensitivity over uninnervated and innervated muscle fibres grown in cell culture. *Devl Biol.* **31**, 147–162.

GINSBORG, B. (1973). Electrical changes in the membrane in junctional transmission. *Biochim. biophys. Acta* **300**, 289–317.

HARTZELL, H. C. & FAMBROUGH, D. M. (1972). Acetylcholine receptors. Distribution and extrajunctional density in rat diaphragm after denervation correlated with acetylcholine sensitivity. *J. gen. Physiol.* **60**, 248–262.

HARTZELL, H. C. & FAMBROUGH, D. M. (1973). Acetylcholine receptor production and incorporation into membranes of developing muscle fibres. *Devl Biol.* **30**, 153–165.

HARTZELL, H. C., KUFFLER, S. & YOSHIKAMI, D. (1975). Post-synaptic potentiation: interaction between quanta of acetylcholine at the skeletal neuromuscular synapse. *J. Physiol.* **251**, 427–463.

KARLIN, A. (1967). On the application of 'a plausible model' of allosteric proteins to the receptor for acetylcholine. *J. theor. Biol.* **16**, 306–320.

KATZ, B. & MILEDI, R. (1972). The statistical nature of the acetylcholine potential and its molecular components. *J. Physiol.* **244**, 665–699.

KATZ, B. & THESLEFF, S. (1957). A study of the 'desensitization' produced by acetylcholine at the motor end-plate. *J. Physiol.* **138**, 63–80.

KIDOKORO, Y. & HEINEMANN, S. (1974). Synapse formation between clonal muscle cells and rat spinal cord explants. *Nature, Lond.* **252**, 593–594.

KONIGSBORG, I. (1963). Clonal analysis of myogenesis. *Science, N.Y.* **140**, 1273–1284.

KUFFLER, S. & YOSHIKAMI, D. (1975). The distribution of acetylcholine sensitivity at the post-synaptic membrane of vertebrate skeletal twitch muscles: iontophoretic mapping in the micron range. *J. Physiol.* **244**, 703–730.

LAND, B. R., SASTRE, A. & PODLESKI, T. R. (1973). Tetrodotoxin-sensitive and insensitive action potentials in myotubes. *J. cell. comp. Physiol.* **82**, 497–510.

MILLER, M. M. & REVEL, J.-P. (1975). Scanning electron microscopy of epithelia prepared by blunt dissection. *Anat. Rec.* **183**, 339–357.

RANG, H. (1971). Drug receptors and their function. *Nature, Lond.* **231**, 91–96.

RITCHIE, A. & FAMBROUGH, D. M. (1975). Electrophysiological properties of the membrane and acetylcholine receptor in developing rat and chick myotubes. *J. gen. Physiol.* **66**, 327–355.

SALPETER, M. M. & BACHMANN, L. (1964). Autoradiography with the electron microscope: a procedure for improving resolution, sensitivity and contrast. *J. cell Biol.* **22**, 469–477.

SALPETER, M. M. & BACHMANN, L. (1972). Electron microscope autoradiography. In *Principles and Techniques of Electron Microscopy. Biological Applications*, vol. 2, ed. HAYAT, M. A., pp. 221–278. New York: Van Nostrand Reinhold.

SALPETER, M. H., FERTUCK, H. C. & SALPETER, E. E. (1977). Resolution in electron microscope autoradiography. III. Iodine-125, the effect of heavy metal staining, and a reassessment of critical parameters. *J. cell Biol.* **72**, 161–173.

STEINBACH, J. H. (1975). Acetylcholine responses on clonal myogenic cells *in vitro*. *J. Physiol.* **247**, 393–405.

STEINBACH, J. H., HARRIS, A. J., PATRICK, J., SCHUBERT, D. & HEINEMANN, S. (1973). Nerve-muscle interaction *in vitro*. Role of acetylcholine. *J. gen. Physiol.* **62**, 255–270.

SYTKOWSKI, A., VOGEL, Z. & NIRENBERG, M. (1973). Development of acetylcholine receptor clusters on cultured muscle cells. *Proc. natn. Acad. Sci. U.S.A.* **70**, 270–274.

YAFFE, D. (1968). Retention of the differentiation potentialities during prolonged cultivation of myogenic cells. *Proc. natn. Acad. Sci. U.S.A.* **61**, 477–483.

YAFFE, D. (1971). Developmental changes preceding cell fusion during muscle differentiation *in vitro*. *Expl Cell Res.* **66**, 33–48.

EXPLANATION OF PLATES

PLATE 1

A, *B* and *C*, light autoradiographs of L6 and primary myotubes. Parts *A* and *B* are two primary myotubes. Note the hot spot in *B*. Part *C* is an L6 myotube. × 720. *D*, scanning EM picture of myotube surrounded by myoblasts. Note the smooth surface of the myotube at this magnification (× 5000).

PLATE 2

Transmission electron microscope autoradiogram of primary myotube. Note that most grains are on the myotube surface. The BTX binding conditions were the same as for the light autoradiographs. The membrane appears essentially smooth at this resolution. × 9600.

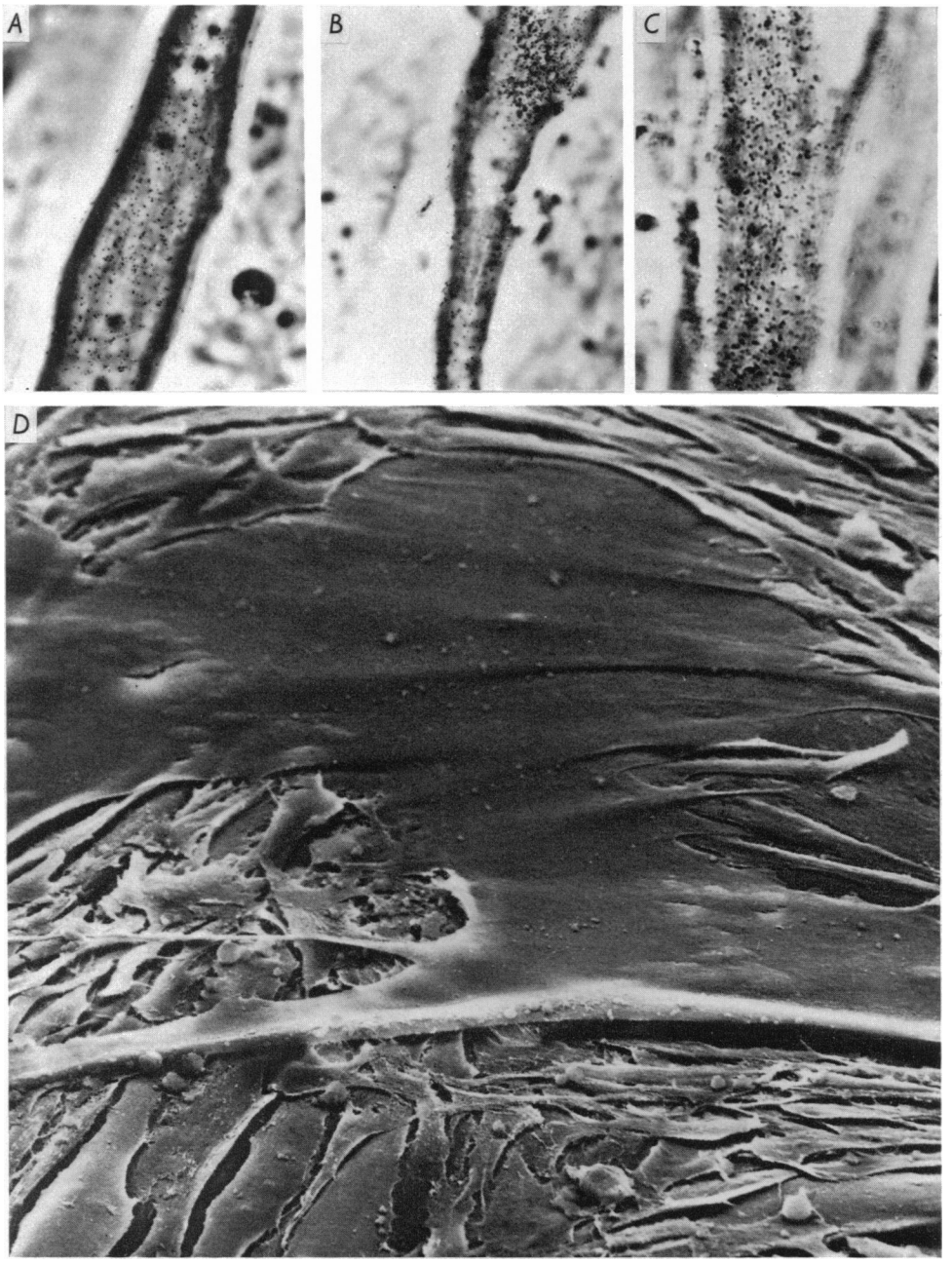

(*Facing p.* 176)